RSC Advances

PAPER

Atomic layer deposition of Al$_2$O$_3$ process emissions†

Lulu Ma, Dongqing Pan, Yuanyuan Xie and Chris Yuan*

The ALD process emissions and the associated chemical reaction mechanism in the ALD of the Al$_2$O$_3$ system are studied and reported. In gaseous emissions, 3.22 vol% of CH$_4$ and 6.01×10^{-2} vol% of C$_2$H$_6$ are found. Net peak emissions of aerosols are found between 1×10^3 and 1×10^4 # cm^{-3} and net total emissions of 25 cycles are in the range of 6.0×10^5 and 2.5×10^6 particles. Most aerosols are determined as ultrafine particles with diameter smaller than 100 nm. Purging time has significant impacts on emission concentrations but no effect on size distribution. Both main and side chemical reactions are observed in the ALD system. X-ray photoelectron spectroscopy (XPS) shows that besides O−Al which represents the existence of Al$_2$O$_3$, a significant amount of C-containing by-products are also generated. Chemical bonds observed in C-containing products are C−H, C−O and C=O. The main reactions can be considered stable to a certain extent, while side reactions accelerate along internal tubes and finally exceed the speed of the main reactions near the outlet of the ALD system. These results could help us to understand the potential environmental impacts of ALD nanotechnology and guide the technology's sustainable scale-up in the future.

Introduction

In recent years, atomic layer deposition (ALD) has found a broad array of industrial applications including semiconductors,[1,2] solar cells,[3,4] polymers,[5,6] and catalysts.[7] In nature, ALD operates by alternating exposure of a substrate to two or more precursors in a cyclic manner. Advantages of ALD include: (1) thickness of ALD film can be controlled at the atomic scale; (2) deposition can be achieved on complex surfaces; (3) uniform, conformal and pinhole-free nano-scale thin films can be fabricated. ALD technology can be used to deposit a wide variety of materials. Usually ALD of Al$_2$O$_3$ is studied as the model process of ALD technology. In this process, Al$_2$O$_3$ thin film is usually obtained through a binary reaction of H$_2$O and trimethylaluminum (TMA) with a typical growth rate of 1 Å per cycle.[8] The overall reaction in ALD of Al$_2$O$_3$ can be described as:

$$2Al(CH_3)_3 + 3H_2O \rightarrow Al_2O_3 + 6CH_4, \Delta H = -376 \text{ kcal}$$
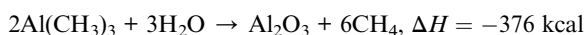
ALD is a self-limited process and only a small portion of the precursors loaded into ALD chamber is deposited on the substrate, while a large portion is discarded as wastes and emissions.[9] Past ALD research was focused on ALD technology development. There are few researches on ALD process

emissions and its relevant environmental impacts. As per the reaction mechanism in ALD process, theoretical emissions are TMA, Al$_2$O$_3$, CH$_4$ and some intermediate reactants. Once released into atmosphere, they can generate certain environmental impacts and also pose potential risks of exposure to both occupational and public health. For instance, CH$_4$ is a flammable and a major greenhouse gas.[10] Global warming potential of CH$_4$ is 25 times higher than that of CO$_2$, so it has a much larger greenhouse effect.[11] Intake of Al$_2$O$_3$ through human exposure could cause a series of neuro-toxicity diseases, including reduction of memory, impairment of psychomotor reaction and disorder of emotional balance.[12] As a nano-manufacturing process, ALD of Al$_2$O$_3$ also produces significant amount of aerosol emissions. Aerosols with higher concentrations can cause adverse effects on human health. It is well known that particles smaller than 10 μm are able to penetrate alveolar region of lung. Ultrafine particles, smaller than 100 nm, can penetrate membranes of respiratory system, enter blood and finally arrive in brain through circulatory system.[12,13] While the ALD of Al$_2$O$_3$ process emissions are of grave concerns because of their potential adverse effects on the environment and human health, however, there is no scientific study so far conducting on the process emissions and the behind mechanism from ALD nano-manufacturing process. This paper is to report our experimental results on the ALD process emissions and the findings on the associated chemical reaction mechanism. The results may facilitate understanding of the potential environmental impacts of the ALD nanotechnology and guide its sustainable scale-up for future large-scale industrial applications.

Department of Mechanical Engineering, University of Wisconsin Milwaukee, Milwaukee 53211, USA. E-mail: Cyuan@uwm.edu; Tel: +1-414-229-5639
† Electronic supplementary information (ESI) available. See DOI: 10.1039/c4ra14568b

Experimental methods

Instrumental setup and sample collection

Fig. 1 is a schematic of the ALD system (Savannash 100, Cambridge Nano Tech Inc.). Two precursors: H_2O (ultrapure grade) and trimethylaluminum (TMA, Strem Chemicals Inc.) were exposed into the reaction chamber alternatively, as controlled by two individual diaphragm ALD valves (Swagelok). ALD reactions are performed in cycles. One cycle of ALD reaction has four basic steps: (1) pulse H_2O into reaction chamber; (2) purge the chamber to remove extra H_2O; (3) pulse TMA into reaction chamber; (4) purge the chamber to remove extra TMA. TMA is an extremely flammable chemical and will ignite spontaneously when come in contact with air. Therefore, exposure of TMA in air must be avoided.[14] In our experimental tests, exposure time of both H_2O and TMA was fixed at 0.015 s and purging time was set in the range between 4 and 20 s. 20 sccm of N_2 was used as carrier gas to flow through the system constantly. A stop valve was installed below the reaction chamber to help control gas flow. Stop valve and ALD valves were operated by compressed air. An inner disk heater embedded in the reaction chamber and heating jackets for other components were used to provide appropriate temperature to the system. In this study, temperature inside the reaction chamber was set at 200 °C. ALD valves and exhaust system including stop valve and pipeline were heated to 150 °C. Neither TMA nor H_2O needed to be heated; so cylinders of two precursors were placed in room temperature. A vacuum pump (XDS 10, Edwards Vacuum, Inc.) was installed at the end of the exhaust pipeline to provide a low pressure (about 0.4 Torr) to the whole system and pump out the extra precursors from the chamber.

The ALD process emissions and the emission generation mechanism are systematically investigated along the exhaust pipeline of the ALD system. 10 pieces of Si wafers are prepared as sample holders to collect chemical resultants within the ALD exhaust pipeline. Their locations are labeled in the schematic of instrumental setup in Fig. 1. Sample 1 locates in the center of

the reaction chamber. Sample 2 and 3 are placed in the exhaust pipeline above the stop valve, and sample 4–9 are placed below the stop valve. Sample 10 is placed at the pump outlet under ambient temperature. Purging time between two pulses was set at 8 s. In this study, these silicon samples are exposed to the same ALD process reactions. In order to improve the efficiency of particle collection, particles emitted from vacuum pump are also collected on a piece of TEM grid (TED PELLA, INC., Prod no. 01824) by aerosols sampler (TSI 3089), where charged particles deposited on a piece of conductive grid through electric field.

Emission analysis

Aerosols emitted from ALD reaction were measured directly at outlet of pump without pre-treatment. Concentration of aerosols was measured by ultrafine condensation particle counter (UCPC, TSI 3776). Size distribution was obtained using a scanning mobility particle sizer (SMPS, TSI 3936) which consists of an electrostatic classifier (TSI 3080) and UCPC. Detailed instrument setup is described in ESI.† In this experiment, five different purging times were used at 4 s, 8 s, 12 s, 16 s and 20 s to study their effects on the ALD process emissions.

Gas emissions were collected at the outlet of pump by a sealed Swagelok gas cylinder and analyzed in the ORS lab (Oneida Research Services Inc.). Purging time between pulses was set at 8 s, the same as Si wafer analysis.

Analysis of chemicals deposited on Si wafer

Because Si wafer was not transparent, reflection method was selected for UV-Vis spectroscopy measurement (light source: DT 1000CE, Analytical Instrument Systems, Inc.; detector: SD2000, Ocean Optics, Inc.). A piece of clean Si wafer was used as background and its reflection was set at 100%.

X-ray photoelectron spectroscopy (XPS, HP 5950A ESCA Spectrometer) was used to determine functional groups of depositions. Concentration of each element was provided by energy-dispersive X-ray spectroscopy (EDS, QUANTAX EDS, Bruker Corp.).

Results and discussion

Gaseous emissions

Analysis of the gaseous emissions shows the existence of N_2, CH_4, H_2O and C_2H_6. Concentration of each component is listed in Table 1.

Fig. 1 Schematic of Al_2O_3 ALD system (Savannash 100, Cambridge Nano Tech Inc.).

Table 1 Concentrations of each component in gaseous emission

Component	Concentration in ALD emission (vol%)
N_2	94.98
CH_4	3.10
H_2O	1.86
C_2H_6	6.01×10^{-2}

N_2 has the highest concentration at 94.98 vol% because it is used as carrier gas to flow through the system consistently. The ALD system is airtight. Though compressed air is used to operate stop valve and ALD valves, it is not introduced into the system. Both N_2 and compressed air are in dry grade, so 1.86 vol% of H_2O is from extra H_2O precursor only. CH_4, the theoretical gaseous resultant, has concentration of 3.10 vol%, which is close to the lower flammability limit of CH_4 at 5 vol%.[15] 6.01 $\times 10^{-2}$ vol% of C_2H_6 is also found in the gaseous emission. In the ALD reaction of TMA and H_2O, a small amount of Al–Al is commonly observed in XPS data. This peak is ably reduced by replacing H_2O with O_3.[16] Methyl radicals $CH_3^{\cdot}$ can be generated by reacting TMA with Al.[17] They are highly reactive and form C_2H_6 easily.

Aerosol emissions

Aerosols emissions from the ALD of Al_2O_3 reactions, including net peak emission and net total emissions of 25 cycles, are shown in Fig. 2.

Net peak emission of aerosols is in the range of 8.0×10^3 and 2.6×10^4 # cm^{-3}. The emission decreases with the increase of purging time. Average global aerosol concentration at continental boundary layer was detected in the range of 1×10^3 to 1×10^4 # cm^{-3}.[18] So concentration of aerosols emitted by ALD reaction is 3 to 10 times larger than the average concentration of global aerosols, and thus is a significant source of air pollution. Concentration of net total emissions is in the range of 6.0×10^5 and 2.5×10^6 particles. Net total emissions also decrease with the increase of purging time. Since pulsing time of each precursor is fixed at 0.015 s, the amounts of precursors injected into the reaction chamber per cycle are the same. The drop of total emission at large purging time indicates that more precursors are adsorbed in the ALD pipeline. Once deposited by precipitation, the surface of pipeline will have a larger tendency of further deposition.[19] These precipitations accumulated along ALD pipeline will lower the heat transfer, prevent gas flow and decrease energy efficiency.[19,20]

Though purging time shows a great influence on the number concentration of aerosol emission, it has limited effect on size distribution, as shown in Fig. 3. Size distribution of aerosols locates in the range between 10 and 300 nm regardless of
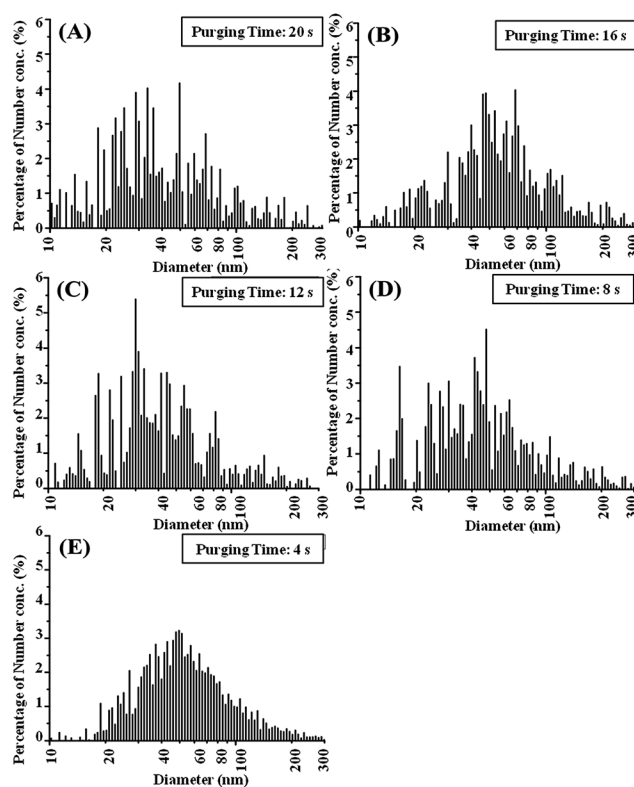

Fig. 2 Net peak emissions of aerosols and net total emission of 25 cycles of ALD reaction measured at pump outlet.

Fig. 3 (A), (B), (C), (D) and (E) are results of size distribution of aerosols emitted at 5 different purging times: 20, 16, 12, 8 and 4 s, respectively.

purging times varying from 4 to 20 s. Most aerosols are ultrafine particles smaller than 100 nm.

UV-Vis analysis of chemicals deposited on Si wafer

To identify the side reactions in the ALD system and identify the emission mechanism from ALD of Al_2O_3 process, components and chemical properties of ALD emissions and the samples installed along internal pipeline are investigated using UV-Vis reflection spectra, XPS and EDS.

Fig. 4 is the UV-Vis reflection spectra of the 10 samples between 300 and 1000 nm. A piece of clean Si wafer is used as background and its reflection is set at 100%. By defining clean Si piece having the first type of UV-Vis spectrum (A), the spectra of the 10 samples can be divided into 3 types: (B), (C) and (D). Type (B), having the smallest reflection at about 350 nm, is observed on sample 1, 2, 4, 5 and 6. Type (C), showing smallest reflection at about 450 nm, is found on sample 3, 8 and 9. (D) is the result of sample #10 collected on the outlet of pump. The optical bandgap of ALD Al_2O_3 film is determined at 6.4 ± 0.1 eV, so it is transparent above 200 nm.[21,22] However, all of the samples in Fig. 4 show significant reflection drop, indicating that chemicals other than Al_2O_3 have been generated and emitted into atmosphere. Reflection curves of sample 1, 2, 4, 5, and 6 decrease gradually from sample 1 to 2 and 4 to 6, respectively with similar spectrum shape. Continuous reflection drop indicates increase of film thickness on Si wafer. Sample 4 is the first sample below the stop valve. Because there is no
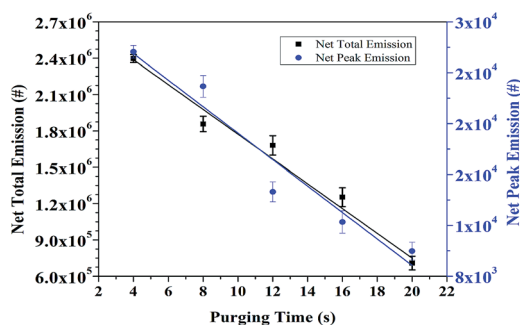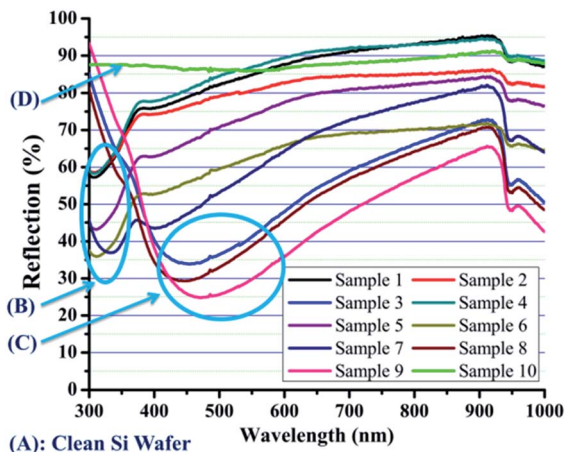
Fig. 4 UV-Vis spectra of the 10 samples inside ALD system.

Fig. 5 XPS data of Carbon. (A), (B), (C) and (D) are correlated with the four types mentioned in Fig. 4.

instrumental component impeding the flow between sample 4 and 9, gas flow is more stable in this region than in the pipeline above stop valve. The shape of reflection curves starts to change from sample 7 and become stable at 8 and 9. Sample 3 is installed above the stop valve but has a similar spectrum as 8 and 9. Reason of this phenomenon is due to the disruption of the stop valve between the sample 3 and 4. Precursors are retarded by it and thus react for a longer time. The change of spectrum curve observed on sample 3, 8 and 9 indicates generation of chemicals that are different from those observed on (B). Sample #10, collected at the outlet of pump, has much higher reflection. Therefore, the mount of emissions of ALD reaction is limited, and most of resultants are adsorbed on the inner wall of the system as precipitations.

XPS analysis of chemicals deposited on Si wafer

Chemical compositions of the four groups of samples are measured by XPS. XPS spectra between 0 and 900 eV is shown in Fig. S2 in the ESI.† Fig. 5 and 6 illustrate detailed C and O spectra, respectively. (A), (B), (C) and (D) are the four types of samples mentioned in Fig. 4. Peaks of C in (B), (C) and (D) are about 3 to 4 times higher compared with that of (A), indicating that significant amounts of C-containing by-products have been generated by ALD reaction. C in (B) exists in the form of C–C/C–H (283.2 eV), C–O (284.8 eV) and C=O (287.2). Meanwhile, three peaks are found in the peak of O: Al–O (530.1 eV), C–O (531.3 eV) and C=O (532.5 eV). Sample (C) also contains C–C/C–H (283.5 eV), C–O (285.0 eV) and C=O (287.6 eV) in the peak of C and Al–O (530.3 eV), C–O (531.4 eV) and C=O (532.4 eV) in the peak of O. However, relative intensity of C–O and C=O in (C) are higher than that in (B). Four peaks of C are observed in sample (D): C–C/C–H (283.6 eV), C–O (285.3 eV), C=O (287.1 eV) and C–F (290.0 eV), where C–F is exhausted by Teflon membrane inside Edwards XDS 10 pump. O in sample (D) is found containing Si–O–Si (531.3 eV), C=O (531.8 eV), Si–O (532.3 eV) and C–O (533.1 eV).[23] Al deposits on the type (B) and (C) is found as Al–O and Al–Al. The results of Al collected on sample (B) and (C) are shown in Fig. 7. A small amount of Al–Al
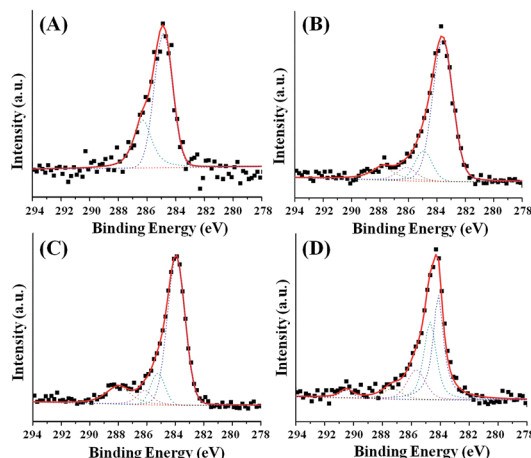
is commonly observed in the reaction of TMA and H_2O, and can be reduced by replacing H_2O with O_3.[16,24] Because efficiency of aerosol collection on Si wafer is limited and density of aerosol distribution is relatively small, no Al is observed on sample (D) by XPS.

Neither H_2O nor N_2 contains C, so TMA is the only source of C. Decomposition of TMA on Si (100) wafer has been observed incompletely.[25] Since the peak of C–Al is not detected, all the TMA has participated in either main or side reactions.[26,27] Reactions of TMA and –OH are able to generate intermediate reactants $(–O)(–OH)Al(CH_3)_2$ and $(–O)_2(–OH)Al(CH_3)$.[28,29] O–O bond is not stable and alkyl peroxide has been found decomposable into ketone and alcohol.[30] Besides generating C_2H_6, $CH_3^{\bullet}$ can react with ROR and generate CH_4 and $ROR^{\bullet}$, where R represents alkyl groups.[31] These radicals can contribute to the formation of C-containing by-products. Since no gas with m/z above 45 is observed, C–O, C=O and O–H containing chemicals are all emitted as aerosols at outlet of the pump.
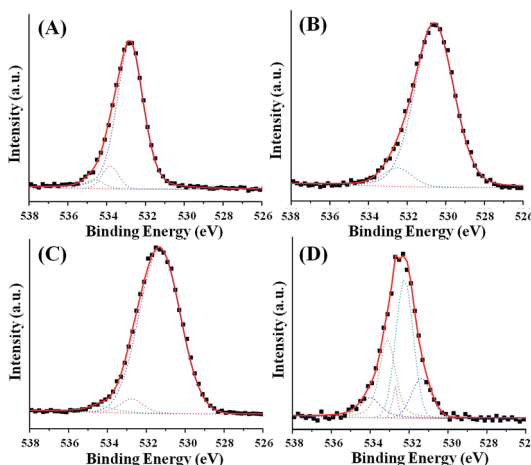

Fig. 6 XPS data of Oxygen. (A), (B), (C) and (D) are correlated with the four types mentioned in Fig. 4.
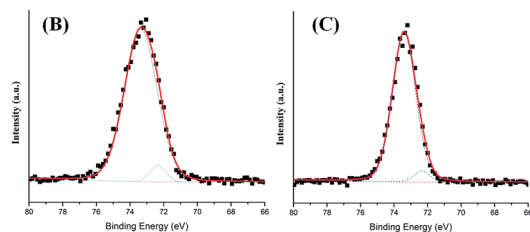
Fig. 7 XPS data of Al. (B) and (C) are correlated with the two types mentioned in Fig. 4.

EDS analysis of chemicals deposited on Si wafer

Measurements of atomic concentration of the 10 samples are also accomplished by EDS. The results are listed in Table S1 in the ESI.† Among these 10 samples, samples 4 to 9 locate in a relatively stable region. Sample 4 has higher concentration of carbon but its UV-Vis spectrum and XPS data are similar with other samples in type (B). This phenomenon is due to the stop valve installed between sample 3 and 4. C is detected on all the samples, indicating that side reactions are found all over the system. Concentration of Al from sample 5 to 9 does not change significantly, while concentrations of C and O both increase gradually. Therefore, reaction that generates Al_2O_3 is stable to a certain extent, while side reactions that generate C-containing chemicals accelerate along the pipeline. At the lower part of system, where sample 8 and 9 are placed, there are more C-containing chemicals generated than Al-containing chemicals. EDS measured on particles collected on TEM grid shows that $4.40 \pm 1.00\%$ of Al, $3.31 \pm 1.07\%$ of C, $83.46 \pm 16.11\%$ of Cu, $4.96 \pm 0.96\%$ of F and $3.86 \pm 0.74\%$ of O are containing in emitted particles.

Conclusions

Both gaseous emissions and aerosols from ALD of Al_2O_3 process are investigated and reported. In the measurement of gaseous emission, CH_4 and C_2H_6 are found generated by ALD reactions, where CH_4 is the second concentrated component in the gaseous emission. Large amounts of aerosols that are 3 to 10 times more concentrated than average global aerosols are generated. Most of them are in the ultrafine range with diameter smaller than 100 nm. Purging time has no effects on aerosol size distribution, but significantly impacts the total net emission of aerosols. In a longer purging time, more aerosols are adsorbed on system pipeline as precipitation. Series measurements of samples collected along ALD exhaust system reflected the emission generation mechanism from both main and side chemical reactions. Aerosols emitted from the ALD reactions have both Al-containing and C-containing compounds, where C-containing compounds are generated through side reactions. XPS shows that chemical bonds, including C–H, C–O and C=O, are contained in by-products. The main reactions can be considered stable to a certain extent, while side reactions accelerate and exceed the speed of main reactions at the last three samples.

Notes and references

1 M. Huang, Y. Chang, C. Chang, Y. Lee, P. Chang, J. Kwo, T. Wu and M. Hong, *Appl. Phys. Lett.*, 2005, **87**, 252104.

2 P. Ye, B. Yang, K. Ng, J. Bude, G. Wilk, S. Halder and J. Hwang, *Appl. Phys. Lett.*, 2005, **86**, 063501.

3 X. Gao, J. Chen and C. Yuan, *J. Power Sources*, 2013, **240**, 503–509.

4 X. Gao, D. Guan, J. Huo, J. Chen and C. Yuan, *Nanoscale*, 2013, **5**, 10438–10446.

5 S. George, *Chem. Rev.*, 2010, **110**, 111–131.

6 E. Langereis, M. Creatore, S. Heil, M. van de Sanden and W. Kessels, *Appl. Phys. Lett.*, 2006, **89**, 081915.

7 M. Pellin, P. Stair, G. Xiong, J. Elam, J. Birrell, L. Curtiss, S. George, C. Han, L. Iton, H. Kung, M. Kung and H. Wang, *Catal. Lett.*, 2005, **102**, 127–130.

8 J. Koo, S. Kim, S. Jeon and H. Jeon, *J. Korean Phys. Soc.*, 2006, **48**, 131–136.

9 J. Huo, X. Lin and C. Yuan, *Proceedings of 2012 ASME Manufacturing Science and Engineering Conference*, Notre Dame, Indiana, USA, June 4–8, 2012.

10 D. Lashof and D. R. Ahuja, *Nature*, 1990, **344**, 529–531.

11 P. Forster, V. Ramaswamy, P. Artaxo, T. Berntsen, R. Betts, D. Fahey, J. Haywood, J. Lean, D. Lowe, G. Myhre, J. Nganga, R. Prinn, G. Raga, M. Schulz and R. Van Dorland, Changes in Atmospheric Constituents and in Radiative Forcing. In Climate Change 2007: The Physical Science Basis, *Contribution of Working Group I to the Fourth Assessment Report of the Intergovernmental Panel on Climate Change*, ed. S. Solomon, D. Qin, M. Manning, Z. Chen, M. Marquis, K. Averyt, M. Tignor and H. Miller, Cambridge University Press, Cambridge, United Kingdom and New York, NY, USA, 2007, pp. 210–216.

12 D. Krewski, R. Yokel, E. Nieboer, D. Borchelt, J. Cohen, J. Harry, S. Kacew, J. Lindsay, A. Mahfouz and V. Rondeau, *J. Toxicol. Environ. Health, Part B*, 2007, **10**, 1–269.

13 U. Pöschl, *Angew. Chem., Int. Ed.*, 2005, **44**, 7520–7540.

14 *Trimethylaluminum; MSDS No. 98-4003*, Strem Chemicals, Inc, Newburyport, MA, April 21, 2011.

15 K. Cashdollara, I. Zlochowera, G. Greena, R. Thomasa and M. Hertzberg, *J. Loss Prev. Process Ind.*, 2000, **13**, 327–340.

16 J. Kim, D. Kwon, K. Chakrabarti, C. Lee, K. Oh and J. Lee, *J. Appl. Phys.*, 2002, **92**, 6739.

17 D. Squire, C. Dulcey and M. Lin, *J. Vac. Sci. Technol., B: Microelectron. Process. Phenom.*, 1985, **3**, 1513.

18 D. Spracklen, K. Carslaw, J. Merikanto, G. Mann, C. Reddington, S. Pickering, J. Ogren, E. Andrews, U. Baltensperger, E. Weingartner, M. Boy, M. Kulmala, L. Laakso, H. Lihavainen, N. Kivekäs, M. Komppula, N. Mihalopoulos, G. Kouvarakis, S. Jennings, C. O'Dowd,

W. Birmili, A. Wiedensohler, R. Weller, J. Gras, P. Laj, K. Sellegri, B. Bonn, R. Krejci, A. Laaksonen, A. Hamed, A. Minikin, R. Harrison, R. Talbot and J. Sun, *Atmos. Chem. Phys.*, 2010, **10**, 4775–4793.

19 K. Hyllestad, Scaling of Calcium Carbonate on a Heated Surface in a Flow Through System with Mono Ethylene Glycol, M.S. thesis, Norwegian University of Science and Technology, Trondheim, Norway, 2008.

20 M. Crabtree, D. Eslinger, P. Fletcher, M. Miller, A. Johnson and G. King, *Oilfield Rev.*, 1999, **11**, 30–45.

21 G. Dingemans and W. Kessels, *J. Vac. Sci. Technol., A*, 2012, **30**, 040802.

22 G. López, P. Ortega, C. Voz, I. Martín, M. Colina, A. Morales, A. Orpella and R. Alcubilla, *Beilstein J. Nanotechnol.*, 2013, **4**, 726–731.

23 A. Namiki, K. Tanimoto, T. Nakamura, N. Ohtake and T. Suzaki, *Surf. Sci.*, 1989, **222**, 530–554.

24 T. Kubo, J. Freedsman, Y. Iwata and T. Egawa, *Semicond. Sci. Technol.*, 2014, **29**, 045004.

25 T. Gow, R. Lin, L. Cadwell, F. Lee, A. Backman and R. Masel, *Chem. Mater.*, 1989, **4**, 406–411.

26 M. Bou, J. Martin and T. LeMogne, *Appl. Surf. Sci.*, 1991, **47**, 149–161.

27 C. Hinnen, D. Imbert, J. Siffre and P. Marcus, *Appl. Surf. Sci.*, 1994, **78**, 219–231.

28 A. Delabie, S. Sioncke, J. Rip, S. Elshocht, G. Pourtois, M. Mueller, B. Beckhoff and K. Pierloot, *J. Vac. Sci. Technol., A*, 2012, **30**, 01A127.

29 B. Gongand and G. Parsons, *J. Mater. Chem.*, 2012, **22**, 15672.

30 N. Kornblum and H. DeLaMare, *J. Am. Chem. Soc.*, 1951, **73**, 880–881.

31 P. Gray and A. Herod, *Trans. Faraday Soc.*, 1986, **64**, 2723–2734.